Bioorganic & Medicinal Chemistry 21 (2013) 6063–6068

Contents lists available at ScienceDirect

Bioorganic & Medicinal Chemistry

journal homepage: www.elsevier.com/locate/bmc

Enantioselective binding of chiral 1,14-dimethyl[5]helicene–spermine ligands with B- and Z-DNA ☆

Genichiro Tsuji, Kyoko Kawakami, Shigeki Sasaki *

Graduate School of Pharmaceutical Sciences, Kyushu University, 3-1-1 Maidashi, Higashi-ku, Fukuoka 812-8582, Japan

ARTICLE INFO

Article history:
Received 11 June 2013
Revised 10 July 2013
Accepted 10 July 2013
Available online 18 July 2013

Keywords:
Chiral recognition
Helicene
DNA binding ligand
Surface plasmon resonance
Isothermal titration calorimetry

ABSTRACT

Duplex DNA adopts a right-handed B-DNA conformation under physiological conditions. Z-DNA, meanwhile, has a left-handed helical structure and is in equilibrium with right-handed B-DNA. We recently reported that the bisnaphthyl maleimide–spermine conjugate (**1**) induced a B- to Z-DNA transition with high efficiency at low salt concentrations. It was also found that the bisnaphthyl ligand (**1**) spontaneously transformed into the corresponding [5]helicene derivative (**2**). Because [5]helicene **2** can potentially be chiral and because the chiral discrimination of B- and Z-DNA is also of interest, we became interested in whether enatiomerically pure [5]helicene–spermine conjugates might discriminate the chirality of B- or Z-DNA. In this study, we have demonstrated an efficient synthesis of chiral DNA-binding ligands by the conjugation of a [5]helicene unit with a spermine unit. These chiral helicene ligands exhibited recognition of B- and Z-DNA, with (*P*)-**3** displaying preference for B-DNA and (*M*)-**3** for Z-DNA. The characteristic features of the helicene–spermine ligands developed in this study include two points: the cationic spermine portion produces electrostatic interactions along the phosphate backbone of the minor groove, and the helicene forms complexes in an end-stacking mode. Such binding modes, together with the thermodynamic parameters, account for the mode of chiral recognition of (*P*)- and (*M*)-**3** for B- and Z-DNA.

1. Introduction

Duplex DNA adopts a right-handed B-DNA conformation under physiological conditions. Z-DNA, meanwhile, has a left-handed helical structure and is in equilibrium with right-handed B-DNA. Since its discovery, Z-DNA has attracted attention in regards to its biological functions,[1] its mechanism of transition to B-DNA,[2] and its applications in chemical devices[3] or DNA nanotechnology.[4] Molecules that specifically bind Z-DNA are also of great interest, and many examples have been investigated, including binding proteins such as ADAR[1,5] *anti*-Z-DNA antibodies,[6] the virus E3L protein,[7] chiral metal complexes,[8,9] and organic ligands.[10–12] We recently reported that the bisnaphthyl maleimide–spermine conjugate (**1**) induced a B- to Z-DNA transition with high efficiency at low salt concentrations.[13] It was also found that the bisnaphthyl ligand (**1**) spontaneously transformed into the corresponding [5]helicene derivative (**2**). Because [5]helicene can potentially be chiral and because the chiral discrimination of B- and Z-DNA is also of interest,[14] we became interested in whether enatiomerically pure [5]helicene–spermine conjugates might discriminate the chirality of B- or Z-DNA. Here, we show that the chiral 1,14-dimethyl[5]helicene–spermine ligand (**3**) exhibits recognition of B- and Z-DNA, with (*P*)-**3** displaying preference for B-DNA and (*M*)-**3** for Z-DNA (Fig. 1). We speculate that recognition takes place in the end-stacking binding mode, which is assisted by electrostatic interactions of the cationic spermine part along the phosphate backbone of the minor groove.

2. Results and discussion

2.1. Design and synthesis of chiral 1,14-dimethyl[5]helicene–spermine ligands

The bisnaphthyl maleimide–spermine ligand (**1**) was converted to [5]helicene ligand (**2**) upon standing under visible light at ambient temperature for one week. The (*P*)- and (*M*)-enantiomers of **2** were separated by chiral column chromatography; however, they racemized quickly.[15] Therefore, 1,14-dimethyl[5]helicene[16] ligand **3** was designed to obtain stable enantiomers. As it turned out that the racemic **3** was not separated by chiral column chromatography, enantiomers were separated at an early stage of the synthesis. The synthesis of **3** is summarized in Scheme 1. The Suzuki–Miyaura coupling of 8-methylnaphthalene-2-boronic acid (**5**)[17] with dibromo-maleimide derivative (**4**) produced the bisaryl substituted compound **6**, which was transformed into racemic helicene

* Corresponding author. Tel./fax: +81 92 642 6615.
E-mail address: sasaki@phar.kyushu-u.ac.jp (S. Sasaki).

0968-0896/$ - see front matter © 2013 The Authors. Published by Elsevier Ltd. All rights reserved.
http://dx.doi.org/10.1016/j.bmc.2013.07.022

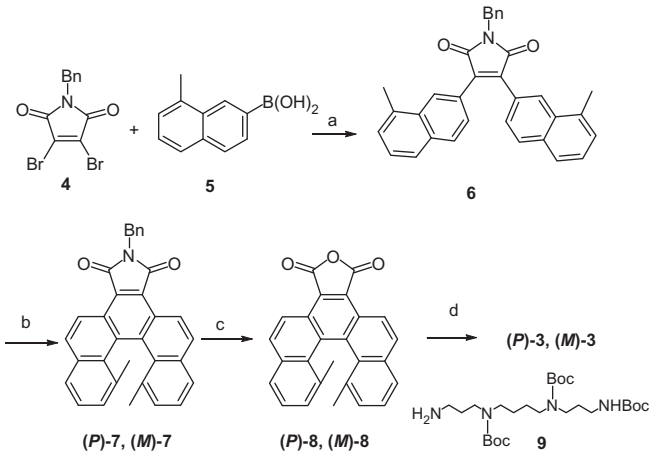

Scheme 1. Reagents and conditions: (a) $PhCH_2NH_3Cl$, $Pd(PPh_3)_2Cl_2$, CsF, H_2O–toluene, 95%; (b) Hg lamp, 500 W, I_2, THF–toluene, 92%; (c) 5 N aq KOH–EtOH, then 10% HCl, 92%; (d) (1) **9**, DMF–toluene; (2) 33% TFA–CH_2Cl_2, 15%.

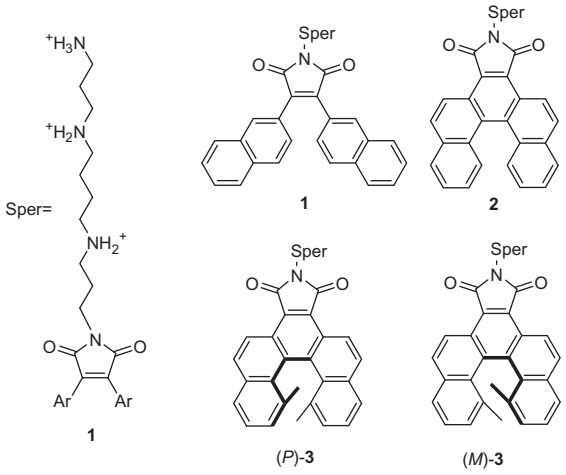

Figure 1. Structures of several spermine-conjugated ligand.

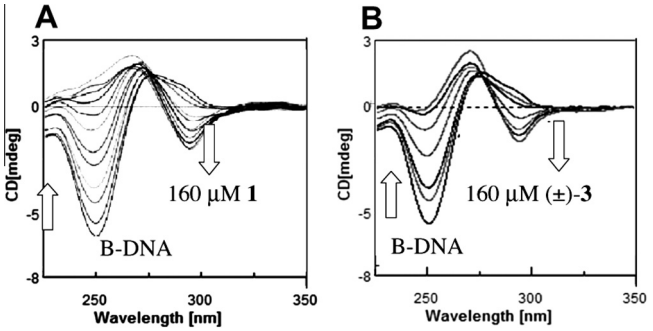

Figure 2. Changes in the CD spectra indicate a B- to Z-DNA transition. (A) In the presence of **1** from 0 to 160 μM; (B) in the presence of (±)-**3** from 0 to 160 μM. An initial CD spectrum was measured using a solution containing 20 μM B-DNA [$d(CGCGCG)_2$] in 5 mM Na cacodylate buffer containing 100 mM NaCl at pH 7.0 and 20 °C. The arrows indicate the direction of change in the spectra effected by the addition of the ligand. The last spectra was obtained in the presence of 160 μM of **1** or (±)-**3**.

Table 1
Effects of the ligands on the T_m and binding constants (K_a) with B- or Z-DNA determined by SPR

Ligand	DNA	ΔT_m[a] °C	K_a, 10^6 M^{-1}[b]	k_a[b], 10^3 M^{-1} s^{-1}	k_d[b], 10^{-3} s^{-1}
1[c]	Z-DNA	+18	3.0	20.2	6.66
1[c]	B-DNA	+16	0.7	5.2	7.49
(*P*)-**3**	Z-DNA	+3.3	0.028	0.163	6.68
(*P*)-**3**	B-DNA	+10.1	0.21	1.72	8.59
(*M*)-**3**	Z-DNA	+7.5	0.22	1.17	5.48
(*M*)-**3**	B-DNA	+4.5	0.11	0.406	3.70

[a] UV-melting temperature was measured using 5 μM B- or Z-DNA in 5 mM Na cacodylate buffer containing 100 mM NaCl in the absence and the presence of 5 μM ligand at pH 7.0.
[b] Sensor chips contain 5′-d(TTTTCGCGCG-TTTT-CGCGCG) as loop B-DNA and 5′-d(TTTTCGCm8GCG-TTTT-CGCm8GCG) as loop Z-DNA. Association constants (K_a) were obtained at 25 °C using a solution of ligand in 5 mM Na cacodylate buffer containing 100 mM NaCl at pH 7.0.
[c] Data obtained from the literature and kinetic parameters were recalculated using the reported sensorgrams.[13]

derivative **7** in 92 % yield as a sole product via a photocyclization reaction in the presence of iodine.[18] The [5]helicene structure is represented by the downfield shift of the protons at 6 and 9 position at 9.02 ppm (doublet, J = 8.6 Hz). (*P*)- and (*M*)-**7** were efficiently separated using a chiral column (OJ-RH) (Fig. 6A), and each enantiomer was transformed into thecorresponding maleic anhydride (**8**). Tri-Boc-protected spermine **9** reacted with **8** to form the corresponding imide derivative, which was treated with TFA to induce the deprotection of the Boc groups, thus producing the helicene–spermine conjugate (**3**). The optical active **8** was returned to **7** by the similar reaction conditions without racemization, indicating that the final helicene–spermine conjugate (**3**) was obtained in optically pure form. Racemic **7** was also converted to the corresponding spermine conjugate (±)-**3** (Scheme 1).

2.2. Stabilization effects of ligands on B- and Z-DNA

The CD spectrum of B-DNA with sequence $d(CGCGCG)_2$ showed a negative band at approximately 255 nm and a positive band at approximately 275 nm. This spectrum changed at high salt concentrations (5 M NaCl) to a CD spectrum with a positive band at approximately 270 nm and a negative band at approximately 295 nm, indicating a B- to Z-DNA transition. It was shown that racemic **3** caused B- to Z-DNA transitions at low salt concentrations (Fig. 2). As the CD bands in the spectra of (*P*)- and (*M*)-**3** overlapped with those of B- and Z-DNA (Fig. 6), these transitions were not similarly evaluated. Accordingly, the chiral recognition of B- or Z-DNA by (*P*)- or (*M*)-**3** was investigated by measuring the thermal denaturing temperature (T_m) and binding affinity (K_a).

As 2′-deoxy-8-methylguanosine (m^8G) is known to stabilize Z-DNA, a duplex containing m^8G, that is, $d(CGCm^8GCG)_2$, was used as a Z-DNA standard.[19] T_m values were obtained by measuring the UV-melting curves of B- and Z-DNA, and the values were obtained in the presence and absence of ligand. The ligands increased the T_m values, as summarized in Table 1. Ligand **1** increased the T_m values of both B- and Z-DNA to a similar extent.[13] Interestingly, (*P*)-**3** increased theT_m value of B-DNA more than that of Z-DNA, whereas its enantiomer (*M*)-**3** had a greater effect on the T_m value of Z-DNA. The selectivities of (*P*)-**3** to B-DNA and (*M*)-**3** to Z-DNA were further evaluated by surface plasmon resonance (SPR) (Fig. 3). 5′-Biotin-conjugated 5′-d(TTTTCGCGCG-TTTT-CGCGCG) (loop B-DNA) and 5′-d(TTTTCGCm8GCG-TTTT-CGCm8GCG) (loop Z-DNA) were immobilized onto a sensor chip as B- and Z-DNA, respectively.[13] The thymidine tetramer (T4) at the 5′-end served as a spacer between the duplex and the sensor surface, and the T4 in the middle allowed for the stem loop of the intramolecular duplex formation.The B- and Z-conformations of each duplex were confirmed by their CD spectra in solution, and loop B-DNA did not

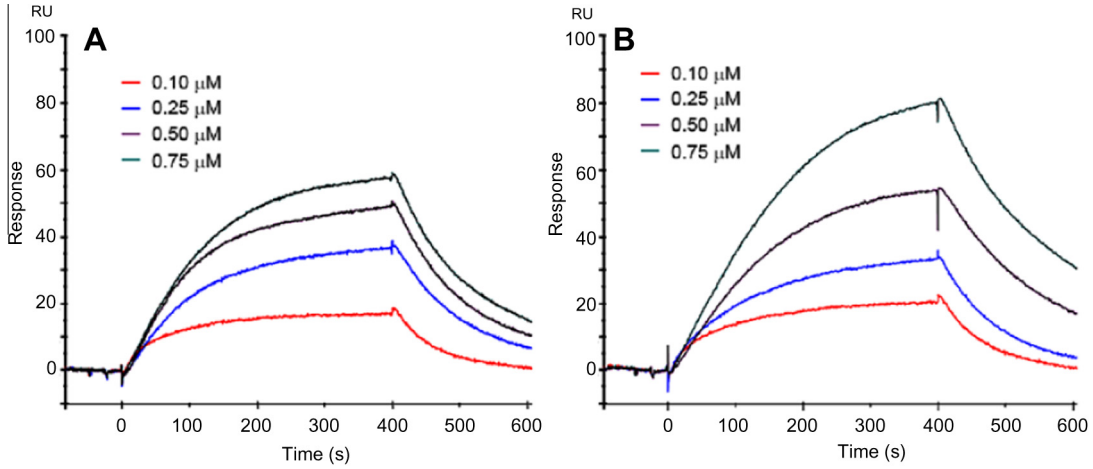

Figure 3. SPR sensorgrams obtained using a chip immobilized with loop DNA. (A) (*M*)-**3** to loop B-DNA; (B) (*M*)-**3** to loop Z-DNA. The SPR spectrum was obtained using a ligand solution in 5 mM Na cacodylate buffer containing 100 mM NaCl at 25 °C, pH 7.0 and a flow rate of 20 μL/min. Kinetic parameters were obtained using manufacturer supplied software, and summarized in Table 2.

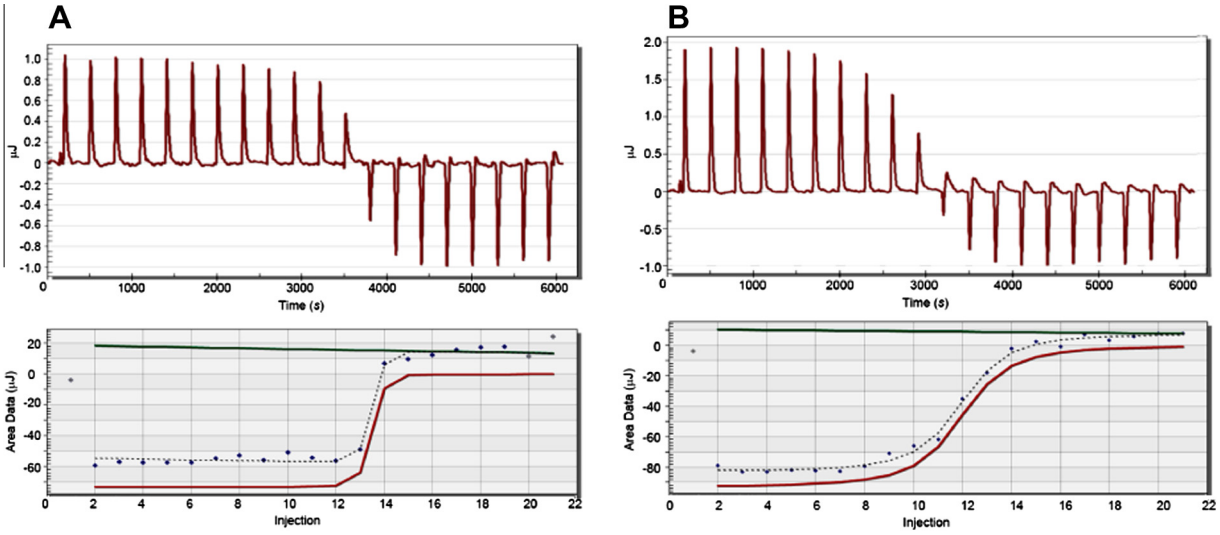

Figure 4. Unsubtracted calorimetric binding heats and binding isotherm obtained from the titration of (*P*)-**3**. (A) Binding to B-DNA. (B) Binding to Z-DNA. Data were obtained using a solution of 10 μM B-DNA or Z-DNA in 5 mM Na cacodylate, 100 mM NaCl at pH 7.0 and 25.0 °C.

change to the corresponding Z-conformation at the ligand concentrations used in these measurements. Examples of SPR sensorgrams are shown in Figure 3. The binding parameters are summarized in Table 1. (*P*)-**3** Showed more than 7 times higher affinity for B-DNA than Z-DNA. In contrast, (*M*)-**3** displayed 2 times higher affinity for Z-DNA. These data are in good agreement with the preferences observed by UV-melting experiments. The kinetic parameters suggest that a larger k_a value contributes to a selectivity of (*P*)-**3** to B-DNA and (*M*)-**3** to Z-DNA. As it seemed to us that-detailed interpretation of the binding mechanism was difficult based on the SPR data, we next investigated binding by isothermal calorimetry (ITC) measurements.

A solution of the ligand (*P*)- or (*M*)-**3** was added to a solution of $d(CGCGCG)_2$ as B-DNA or $d(CGCm^8GCG)_2$ as Z-DNA, and binding isotherms were obtained. Figure 4 illustrates examples obtained from the titration of (*P*)-**3**. The obtained K_a values and thermodynamic parameters are summarized in Table 2. An analysis of the binding heats obtained from the titration of (*P*)-**3** to B-DNA indicated a DNA:ligand = 2:1 ratio of complexation with an association constant of $K_a = 3.7 \times 10^8\ M^{-1}$, indicating high-affinity binding between (*P*)-**3** and B-DNA (Fig. 4A). This affinity is 50 times greater than the complexation between (*P*)-**3** and Z-DNA (Fig. 4B), again confirming the preference of (*P*)-**3** for B-DNA. A preference of (*M*)-**3** for Z-DNA was also observed by ITC measurements with two times higher affinity than binding to B-DNA (Table 2).

Table 2
Thermodynamic parameters obtained by ITC using (*P*)- and (*M*)-**3** against B- and Z-DNA[a]

Complex to B- or Z-DNA	K_a, $10^7\ M^{-1}$	N[b]	ΔH (kJ/mol)	ΔG (kJ/mol)	$-T\Delta S$ (kJ/mol)
1 versus Z[c]	0.31	4.1	−32.6	−37.0	−4.5
1 versus B[c]	0.62	3.5	−21.8	−33.1	−11.3
(*P*)-**3** versus Z	0.67	1.7	−46.6	−38.9	7.7
(*P*)-**3** versus B	36.7	2.0	−36.5	−48.9	−12.4
(*M*)-**3** versus Z	0.17	1.8	−47.7	−35.6	12.1
(*M*)-**3** versus B	0.083	4.0	−23.6	−33.8	−10.2

[a] Thermodynamic parameters were obtained as shown in Figure 4.
[b] The binding stoichiometry is defined as molar ratio [ligand]/[duplex].
[c] Data are taken from the literature.[13] The ΔG and $-T\Delta S$ values were miscalculated in the literature and are corrected in this table.

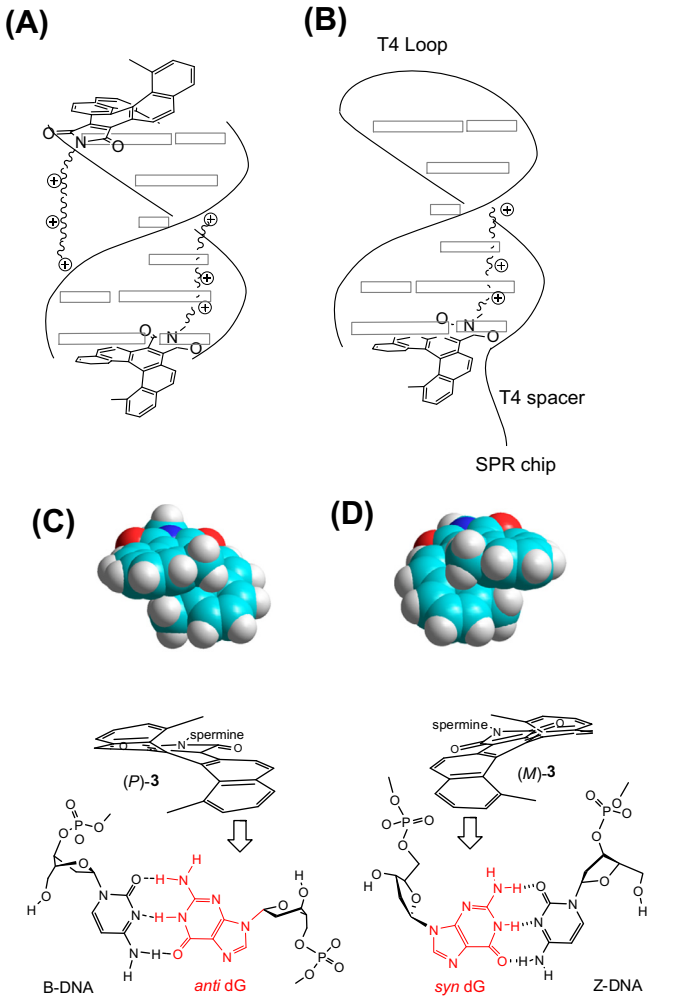

Figure 5. Schematic illustrations of speculative ligand binding. (A) End-stacking mode of the binding with B-DNA; (B) T4 loop and T4 spacer inhibit end-stacking binding; (C) Space-filling model of (*P*)-**3** and its schematic binding mode to a dG in *anti* conformation; (D) Space filling model of (*M*)-**3** and its speculative binding to a dG in *syn* conformation at the end of the Z-DNA. The spermine moiety has been omitted from the space-filling model for clarity.

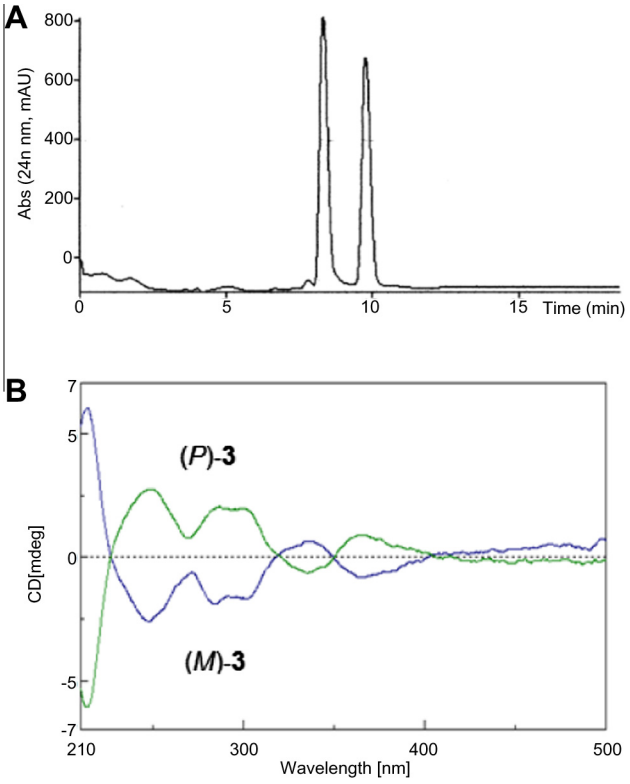

Figure 6. (A) The HPLC Chart of (*M*)-**7** and (*P*)-**7** separated by OJ-RH. Column DAICEL OJ-RH column (4.6 mmφ × 150 mm), solvent CH_3CN, flow rate of 0.500 mL/min, 35 °C. (A) Faster peak at 8.3 min and a peak at 9.8 min correspond to (*M*)-**7** and (*P*)-**7**, respectively; (B) CD Spectra of (*P*)-**3** (green line) and (*M*)-**3** (blue line). Spectra were obtained using a 10 μM ligand solution in 5 mM Na Cacodylate buffer containing 100 mM NaCl at pH 7.0 and 20 °C.

Examination of the thermodynamic parameters indicates that the binding of (*P*)-**3** and B-DNA is an enthalpically and entropically favorable process. In contrast, the binding of (*P*)-**3** with Z-DNA is enthalpically favorable, but it is associated with an unfavorable change in entropy ($-T\Delta S$ = 7.7 kJ/mol) and results in a low binding affinity. For (*M*)-**3**, although binding with B-DNA is also enthalpically and entropically favorable, the enthalpy contribution is relatively small (ΔH = −23.6 kJ/mol). The binding of (*M*)-**3** with Z-DNA is associated with an unfavorable entropy term ($-T\Delta S$ = 12.1 kJ/mol), but a large enthalpic contribution (ΔH = −47.7 kJ/mol) compensates to produce the observed selectivity for Z-DNA. The K_a values obtained by ITC were larger than those obtained by SPR. Based on the NMR measurements obtained in the previous study,[13] the binding of **1** with duplex DNA contains a stacking mode at the ends of the duplex. The importance of an end stacking interaction for Z-DNA has also been suggested in other study.[20] The stoichiometry of the binding of (*P*)-**3** with B- or Z-DNA was estimated to be ligand:DNA = 2:1, suggesting that (*P*)-**3** binds the duplex in an end-stacking mode, as illustrated in Figure 5A.

We speculate that an end-stacking binding mode such as shown in Figure 5A is assisted by electrostatic interactions of the cationic spermine part along the phosphate backbone of the minor groove. This notion is partly supported by the fact that more than 100-fold smaller K_a values were obtained by SPR because end-stacking interactions should be hampered by steric hindrance of a T4 loop on one side. Also, the T4 spacer most likely causes an additional steric hindrance (Fig. 5B). In such an end-stacking complex, the positive helix face of (*P*)-**3** seems to interact with dG preferably in an *anti*-conformation, as schematically shown in Figure 5C. X-ray analysis of a crystalline complex between $d(CGCGCG)_2$ with a polyamine has shown that polyamines bind in the minor groove of the Z-form of $d(CGCGCG)_2$.[21] The minor groove of Z-DNA is narrower than that of B-DNA. The binding of the cationic spermine portion of (*P*)-**3** in the minor groove would produce higher electrostatic interactions for a favorable enthalpy effect. Meanwhile, the limited degrees of freedom of the spermine portion can cause a loss of entropy. Thus, the low affinity of (*P*)-**3** to Z-DNA is rationalized in terms of favorable enthalpy and unfavorable entropy. The binding of (*M*)-**3** to Z-DNA may be considered based on the formation of a similar complex as follows: a negative helical face of (*M*)-**3** is preferable for end-stacking with dG in the *syn* conformation of Z-DNA, as illustrated in Figure 5D. On the contrary, enthalpic contributions during the binding of (*M*)-**3** to B-DNA decreased largely (ΔH = −23.6 kJ/mol), most likely due to fewer end-stacking interactions between a negative helical face of (*M*)-**3** and the dC–dG base pair at the end of B-DNA, thus resulting in the selectivity of (*M*)-**3** for Z-DNA.

3. Conclusion

In this study, we have demonstrated an efficient synthesis of chiral DNA-binding ligands by the conjugation of a [5]helicene unit

with a spermine unit. These chiral helicene ligands exhibited recognition of B- and Z-DNA, with (*P*)-**3** displaying preference for B-DNA and (*M*)-**3** for Z-DNA. Although several studies have claimed chiral recognition of B- and Z-DNA, the modes of this chiral recognition remain poorly understood. The characteristic features of the helicene–spermine ligands developed in this study include two points: the cationic spermine portion produces electrostatic interactions along the phosphate backbone of the minor groove, and the helicene forms complexes in an end-stacking mode. Such binding modes, together with the thermodynamic parameters, account for the mode of chiral recognition of (*P*)- and (*M*)-**3** for B- and Z-DNA. The results of this study may provide useful knowledge for designing small molecular ligands for the recognition of B- or Z-DNA.

4. Experimental section

^{1}H NMR spectra were recorded at 400 MHz on a Varian 400 UNITY using $CDCl_3$, CD_3OD, CD_3CN or D_2O as a solvent. ^{13}C NMR spectra were recorded at 125 MHz on a Varian INOVA 500 using D_2O as a solvent. Chemical shifts are reported in ppm, in δ units. ESI-MS spectra were recorded on an Applied Biosystems Marinar System 5299 API-TOF instrument. IR spectra were recorded on a PerkinElmer Spectrum One FT-IR spectrometer.

4.1. 1-Methylnaphthalene-7-boronic acid (5)

A solution of *n*-butyl lithium in hexane (1.54 M, 1.9 mL, 2.94 mmol) was added into a solution of 7-bromo-1-methylnaphthalene (0.59 g, 2.67 mmol) in dry THF (10 mL) at −78 °C, and the mixture was stirred at the same temperature for 1 h. A solution of 2,4,6-trimethoxyboroxin (0.46 mL, 5.34 mmol) in dry THF (10 mL) was dropped into the above solution, and the mixture was stirred for 30 min at the same temperature. The mixture was warmed to 0 °C, stirred for 1 h at the same temperature, and at room temperature for additional 2 h. The mixture was quenched by the addition of 10% aqueous HCl (20 mL), and extracted with ether (20 mL × 2). The organic layers were washed with brine, dried over Na_2SO_4, evaporated. The residue was chromatographed (silica gel, *n*-hexane only to *n*-hexane:AcOEt = 3:1) to give **5** as colorless solids (384 mg, 77%). ^{1}H NMR (400 MHz,$CDCl_3$) δ (ppm) 8.28 (1H, s), 7.87 (1H, dd, *J* = 7.6, 1.8 Hz), 7.82 (1H, d, *J* = 7.6 Hz), 7.38–7.31 (2H, m), 2.78 (1H, s), 2.64 (3H, s). ^{13}C NMR(125 MHz, CD_3OD) δ (ppm) 131.9, 131.2, 130.9, 130,5, 128.4, 127.6, 127.3, 127.2, 127.1, 19.4. ESI–HRMS (*m*/*z*) calcd for $C_{11}H_{10}BO_2$ 185.0781 $[M+H]^-$, found 185.0762.

4.2. Compound 6

1-Benzyl-3,4-dibromopyrrole-2,5-dione(**4**) (0.15 g, 0.435 mmol), **5** (0.24 g, 1.3 mmol), dichlorobis-(triphenylphosphine)palladium(II) (16 mg, 0.022 mmol) and benzyltriethylammonium chloride (5 mg, 0.022 mmol) were dissolved in degassed toluene (4 mL), followed by the addition of CsF (0.265 g, 1.74 mmol) in water (3 mL). The mixture was stirred at 80 °C for 2 h. The mixture was quenched by the addition of saturated aqueous NH_4Cl (20 mL) and extracted with AcOEt (20 mL× 2). The combined organic layers were dried over Na_2SO_4, evaporated. The residue was chromatographed (silica gel, *n*-hexane:AcOEt = 10:1) to give **6** as pale yellow solids (198 mg, 97%). ^{1}H NMR(400 MHz, $CDCl_3$) δ (ppm) 8.38 (2H, s), 7.67(2H, d, *J* = 8.6 Hz), 7.63(2H, d, *J* = 7.9 Hz), 7.52(2H, d, *J* = 7.3 Hz), 7.39(4H, t, *J* = 7.9 Hz), 7.36(2H, d, *J* = 7.3 Hz), 7.35(3H, d, *J* = 7.3 Hz), 7.21–7.13 (2H, m), 4.88(2H, s), 2.57(6H, s). ^{13}C NMR(125 MHz, $CDCl_3$), δ (ppm) 1170.7, 136.6, 136.0, 135.5, 132.3, 128.8, 128.8, 128.8, 128.7, 128.7, 128.6, 127.9, 127.3, 127.2, 42.1, 19.2. IR (cm^{-1}) 1627, 1601, 1208, 823. ESI–HRMS (*m*/*z*) calcd for $C_{33}H_{26}NO_2$ 468.1958 $[M+H]^+$, found 468.1977.

4.3. (*P*)-7 and (*M*)-7

A solution of **6** (10 mg, 0.021 mmol) and iodine (6 mg, 0.024 mmol) in tolunene-THF was stirred under irradiation of high-pressure mercury lamp (500 W) for 6 h. The reaction mixture was quenched with saturated aqueous $Na_2S_2O_3$ (20 mL), and extracted with AcOEt (20 mL × 2). The organic layers were washed with water, brine, and dried over Na_2SO_4, then evaporated. The residue was chromatographed (silica gel, *n*-hexane:toluene = 10:1) to give **7** as yellow solids (9 mg, 92%).

4.4. Optical resolution of (*P*)-7 and (*M*)-7

A solution of racemic **7** was separated by HPLC equipped with a chiral column (DAICEL OJ-RH 4.6 mmφ × 150 mm) using CH_3CN as an eluent at a flow rate of 0.500 mL/min and at 35 °C (Fig. 6A).

IR(cm^{-1}) 1754, 1700, 1389, 1345, 826. $[\alpha]_D^{25}$ ($CHCl_3$) +356.7 (*M*)-**7**, −398.3 (*P*)-**7**. ^{1}H NMR(400 MHz, $CDCl_3$) δ (ppm) 9.02 (2H, d, *J* = 8.6 Hz), 8.04 (2H, d, *J* = 8.6 Hz), 7.87 (2H, d, *J* = 7.9 Hz), 7.56–7.52 (4H, m), 7.32 (2H, t, *J* = 7.3 Hz), 7.27 (1H, d, *J* = 1.2 Hz), 7.10 (2H, d, *J* = 7.3 Hz), 4.98 (2H, s), 0.86 (6H, s). ^{13}C NMR(125 MHz, $CDCl_3$) δ (ppm) 169.4, 136.7, 135.4, 133.7, 131.7, 130.6, 130.5, 129.7, 128.7, 128.5, 127.7, 127.6, 126.0, 125.7, 124.9, 120.6, 41.5, 22.1. ESI–HRMS (*m*/*z*) calcd for $C_{33}H_{23}NO_2$ $C_{33}H_{24}NO_2$ 466.1802 $[M+H]^+$, found 466.1840.

4.5. Synthesis of (*P*)-3

A solution of (*P*)-**7** (0.135 g, 0.290 mmol) in ethanol-5 M aqueous KOH (10−5 mL) was stirred at room temperature for 2 h, then the mixture was acidified with 10% aqueous HCl (20 mL). The precipitates were collected and washed with water, then dried under vaccum to give (*P*)-**8** as orange solids (9 mg, 83%). This material was used for the next reaction without purification. A mixture of **9** (7.3 mg, 0.145 mmol) and (*P*)-**8** (6 mg, 0.159 mmol) in toluene–DMF (3–1 mL) was heated at 80 °C for 16 h. The solvents were evaporated and the residue was chromatographed (silica gel, CH_2Cl_2 to CH_2Cl_2–MeOH = 200:1) to give yellow solids (3.2 mg, 26%). This material was treated with 33% TFA in CH_2Cl_2 (10 mL) at 0 °C for 3 h, and the solvents were evaporated. The crude material was purified by HPLC (nacalai tesque COSMOSIL 5C_{18}-AR-II, 4.6 × 250 mm, solvents 0.05% TFA in water:0.05% TFA in CH_3CN = 60:40) to give (*P*)-**3** as yellow solids (2 mg, 15%). (*M*)-**3** and (±)-**3** were obtained similarly from (*M*)-**7** and (±)-**7**, respectively (Fig. 6B). Concentration of a stock solution of the ligand was determined by NMR integration value using an internal standard. IR(cm^{-1}), 1676, 1202, 1130, 828, 723, $[\alpha]_D^{25}$ (MeOH) +240.3(*M*), −240.6(*P*), ^{1}H NMR(400 MHz, $CDCl_3$) δ (ppm) 8.99 (2H, d, *J* = 8.8 Hz), 8.15 (2H, d, *J* = 8.8 Hz), 7.97 (2H, d, *J* = 1.6 Hz), 7.62 (2H, t, *J* = 7.6 Hz), 7.16 (2H, d, *J* = 6.7 Hz), 3.96 (2H, t, *J* = 6.1 Hz), 3.19 (2H, br), 3.13−3.01 (8H, br), 2.19 (2H, br), 2.08 (2H, br), 1.80 (4H, br), 0.87 (6H, s). ESI–HRMS(*m*/*z*) calcd for $C_{36}H_{41}N_4O_2$ 561.3224 $[M+H]^+$ found 5631.3230.

4.6. DNA oligomers

DNA oligomers were synthesized by the automated DNA synthesizer using the conventional amidite chemistry. The DMTr-protected DNA was cleaved from the resin with NH_4OH solution and purified by HPLC equipped with a ODS column using 0.1 M TEAA−CH_3CN linear gradient system. The DMTr protecting group of the purified ODN was cleaved in 10% aqueous AcOH, and the mixture was washed with ether. The purity of the ODN was

confirmed by MALDI-TOF MS and UV measurements. The concentration of the stock solution was estimated by the UV absorbance at 260 nm, which was further confirmed to be less than 5% error by HPLC analysis of the component nucleosides after enzymatic hydrolysis using BAP and VPDE.

4.7. CD measurement

CD spectra were recorded by a Jasco-J720 spectrometer using a 200 μL 2 mm quartz glass cell at the constant temperature at 20 °C. A solution of $d(CGCGCG)_2$ B-DNA (20 μM) or $d(CGCm^8GCG)_2$ Z-DNA (20 μM) in the buffer (5 mM Na cacodylate containing 100 mM NaCl at pH 7) was used for the CD measurement. The ODN solution was titrated with the ligand stock solution (1 μL each). All CD data were blank corrected, and reported as the average of quadruplicate scans.

4.8. Measurement UV melting temperature

In the UV melting experiments, a solution of Z-DNA (5 μM in Na cacodylate buffer 5 mM containing 100 mM NaCl, pH 7) was used. The temperature was raised or lowered at the rate of 1 °C/min between 10 and 60 °C.

4.9. Surface plasmon resonance (SPR) measurements

5′-Biotin-conjugated d(TTTTCGCGCG-TTTT-CGCGCG) or d(TTTTCGC m^8GCG-TTTT-CGC m^8GCG) 10–500 nM in 10 mM HEPES and 0.15 M NaCl at pH 7.4 was immobilized on a sensor chip SA at 20 °C. One flow channel was always left as a blank for reference. The SPR measurement was performed at 25 °C using the 5 mM Na cacodylate buffer containing 100 mM NaCl at pH 7.0 as the running buffer. Binding was measured at 20 μL/min for 120 s and dissociation for 150 s. A Biacore 3000 (GE Healthcare) was used for the SPR measurements.

4.10. Isothermal titration calorimetry (ITC)

The ligand solution (1 mM **3c**) was prepared by dissolution in the final dialysate obtained from the ODN dialysis, and was titrated into 10.0 μM $d(CGCGCG)_2$ or $d(CGCm8GCG)_2$ in 5 mM Na cacodylate buffer containing 100 mM NaCl at pH 7.0 and 25.0 °C. The first injection was 2 μL and then 10 μL each of the ligand stock was added to the ODN solution. The data obtained by the first injection was omitted from the analysis. The ODN concentrations are reported as molar concentrations of double strands. All samples were degassed prior to use by application of vacuum with simultaneous stirring on a magnetic stir plate. A NanoITC SV (TA Instruments) was used for the calorimetric measurements.

Acknowledgements

This work was supported by a Grant-in-Aid for Scientific Research (S) from the Japan Society for Promotion Science (JSPS).

References and notes

1. Rich, A.; Zhang, S. *Nat. Rev. Genet.* **2003**, *4*, 566.
2. Fuertes, M. A.; Cepeda, V.; Alonso, C.; Pérez, J. M. *Chem. Rev.* **2006**, *106*, 2045.
3. Mao, C.; Sun, W.; Shen, Z.; Seeman, N. C. *Nature* **1999**, *397*, 144.
4. Seeman, N. C.; Belcher, A. M. *Proc. Natl. Acad. Sci. U.S.A* **2002**, *99*(Suppl 2), 6451–6455.
5. Ha, S. C.; Lowenhaupt, K.; Rich, A.; Kim, Y.-G.; Kim, K. K. *Nature* **2005**, *437*, 1183.
6. Lafer, E. M.; Möller, A.; Nordheim, A; Stollar, B. D.; Rich, A. *Proc. Natl. Acad. Sci. U.S.A.* **1981**, *78*, 3546.
7. Kwon, J.-A.; Rich, A. *Proc. Natl. Acad. Sci. U.S.A.* **2005**, *102*, 12759.
8. Wu, Z.; Tian, T.; Yu, J.; Weng, X.; Liu, Y.; Zhou, X. *Angew. Chem., Int. Ed.* **2011**, *50*, 11962.
9. Erkkila, K. E.; Odom, D. T.; Barton, J. K. *Chem. Rev.* **1999**, 2777.
10. Qu, X.; Trent, J. O.; Fokt, I.; Priebe, W.; Chaires, J. B. *Proc. Natl. Acad. Sci. U.S.A.* **2000**, *97*, 12032.
11. Xu, Y.; Zhang, Y. X.; Sugiyama, H.; Umano, T.; Osuga, H.; Tanaka, K. *J. Am. Chem. Soc.* **2004**, *126*, 6566.
12. Honzawa, S.; Okubo, H.; Anzai, S.; Yamaguchi, M.; Tsumoto, K.; Kumagai, I. *Bioorg. Med. Chem.* **2002**, *10*, 3213.
13. Doi, I.; Tsuji, G.; Kawakami, K.; Nakagawa, O.; Taniguchi, Y.; Sasaki, S. *Chem-Eur. J.* **2010**, *16*, 11993.
14. Barton, J. K.; Basile, L. A.; Danishefsky, A.; Alexandrescu, A. *Proc. Natl. Acad. Sci. U.S.A.* **1984**, *81*, 1961.
15. Goedicke, C.; Stegemeyer, H. *Tetrahedron Lett.* **1970**, *11*, 937.
16. Janke, R. H.; Wu, E.; Borkent, J. H. *J. Am. Chem. Soc.* **1996**, *118*, 6031.
17. Singh, I.; Seitz, O. *Organic Lett.* **2006**, *8*, 4319.
18. Harish, R. Talele; Monik, J. Gohil; Ashutosh, V. Bedekar *Bull. Chem. Soc. Jpn.* **2009**, *82*, 1182.
19. Xu, Y.; Ikeda, R.; Sugiyama, H. *J. Am. Chem. Soc.* **2003**, *125*, 13519.
20. Pan, B.; Ban, C.; Wahl, M. C.; Sundaralingam, M. *Biophys. J.* **1997**, *73*, 1553.
21. Ohishi, H.; Odoko, M.; Zhou, D.-Y.; Tozuka, Y.; Okabe, N.; Nakatani, K.; Ishida, T.; Grzeskowiak, K. *Biochem. Biophy. Res. Commun.* **2008**, *368*, 382.